INTERNATIONAL JOURNAL OF CHEMICAL REACTOR ENGINEERING

Volume 6 2008 *Article* A53

Modeling and Development of a Microwave Heated Pilot Plant for the Production of SiC-Based Ceramic Matrix Composites

Beatrice Cioni* Andrea Lazzeri†

*University of Pisa, beatrice.cioni@ing.unipi.it

†University of Pisa, a.lazzeri@ing.unipi.it

ISSN 1542-6580

Modeling and Development of a Microwave Heated Pilot Plant for the Production of SiC-Based Ceramic Matrix Composites*

Beatrice Cioni and Andrea Lazzeri

Abstract

This paper outlines the development of a microwave heated apparatus for the production of silicon carbide (SiC) based ceramic matrix composites via chemical vapor infiltration. An innovative pilot scale reactor was designed and built. A coupled thermal and electromagnetic model was developed in order to predict the temperature profile inside the reactor. The results obtained from the model demonstrated that the electric field inside the sample was constant. This fact is particularly important in order to prevent the thermal instabilities (run-aways) that are typical in the case of microwave heating. Therefore the heating was uniform with the aid of a mode stirrer that achieved a better distribution of the microwave power and then improved the process efficiency. The infiltration cycles were carried out on SiC fiber preforms and resulted in an excellent average weight increase with respect to the initial sample. By using microwave heating, the treatment times were considerably reduced with respect to the conventional process times reported in the literature. The microstructure of the SiC composites were observed by scanning the electron microscopy in order to evaluate the quality and the degree of densification which was achieved within the fiber tows. The SiC deposition inside of the sample was sufficiently homogeneous and compact, even if a certain degree of inter-tow porosity was still evident.

KEYWORDS: microwave, modeling, chemical vapor infiltration, ceramic matrix composites, silicon carbide

---

*The authors would like to thank Francesco Nenciati who made a useful contribution to thermal and electromagnetic modeling and Dr. Giuseppe Gallone for the measurement of the reflection coefficient.

1. Introduction

The importance of minimizing the impact that chemical processing produces on the environment is growing. Optimal use of material and energy, and an efficient waste management can be recognized as important factors for environmental protection. In fact one important element of sustainable chemistry, well-known as *green chemistry*, is commonly defined as the chemical research aiming at the optimization of chemical processes and products with respect to energy and material consumption, inherent safety, toxicity, environmental degradability, and so on (Anastas and Warner, 1998). Microwave processing of materials is a technology that can provide the material processor with a new, powerful, and significantly different tool with which to process materials that may not be amenable to conventional means of processing or to improve the performance characteristics of existing materials. Microwave radiation is, in principle, a clean source of energy since electric power can be produced from renewable resources. More importantly, microwave energy is transferred volumetrically, rather than superficially like in conventional heating, resulting in much fast and efficient heat transfer. Therefore significant energy savings are possible. The most likely candidates for future production-scale applications will be those which will be able to take full advantage of the unique characteristics of microwaves (Sheppard, 1988).

Ceramic matrix composites (CMCs) represent the latest entry in the field of composites for applications involving high temperature and harsh operating conditions, since a major shortfall of conventional ceramics is that they possess a low fracture toughness which can results in brittle failure (Chawla, 1993). CMCs combine the thermal and chemical resistance of monolithic ceramics with the mechanical strength of ceramic reinforcements with an improved fracture toughness when compared with ordinary ceramics. Ceramic matrix composites can be processed according to: (1) a gas phase route, also referred to as chemical vapor infiltration (CVI), (2) a liquid phase route including the polymer impregnation/pyrolysis (PIP), and liquid silicon infiltration (LSI) also called (reactive) melt infiltration (RMI or MI) processes, as well as (3) a ceramic route, i.e. a technique combining the impregnation of the reinforcement with a slurry and a sintering step at high temperature and high pressure.

Conventional ceramic routes to producing CMCs require the use of high temperatures to sinter the individual ceramic particles of the matrix together, but sintering temperatures are typically much higher than the upper temperature limits of the fibers (Chawla, 1993). Recently a new technique, the nano-infiltration and transient eutectic (NITE) process, has been developed for silicon carbide (SiC) ceramic matrix composites primarily for thermo-structural applications (Katoh et al., 2002). NITE SiC_f/SiC composites was developed for reduced porosity,

advanced matrix quality control, and strong fiber–matrix interface (Katoh et al., 2004), but very high temperature of sintering are required (1700-1800°C). So only high thermal stability fibers, for example quasi-stoichiometric SiC fibers prepared at high temperatures [such as Tyranno SA (Ube Industries, Japan) or Sylramic fibers (Dow Corning, USA)] can be employed, in order to avoid fiber damaging. Also there is a certain degree of uncertainty whether a strong fiber-matrix interface is desirable for achieving high fracture toughness.

Among industrially available matrix densification techniques, chemical vapor infiltration (CVI) best meets the quality requirements for CMCs (Besmann et al., 1995), particularly for the production of SiC ceramic reinforced with SiC fibers (SiC_f-SiC composites) that present excellent high temperature properties including: high strength, high modulus of elasticity, low coefficient of thermal expansion, and hence good wear and thermal shock resistance, chemical stability and a greater fracture toughness than for unreinforced SiC. In the gas phase route, the different constituents of the composite, i.e. the interphase, the matrix and the external coating, are successively deposited from gaseous precursors at moderate temperatures (900–1100 °C) and under reduced pressures (or sometimes at the atmospheric pressure).

Advantages of CVI (Lovell, 1991; T.D. Gulden et al., 1990) vs. other fabrication methods, such as hot pressing, for densifying and fabricating composite materials are the following: 1) CVI is a near-net-shape process; 2) CVI minimizes the mechanical damage to the fibers as a result of the much lower pressures and temperatures employed in CVI, compared to those in other fabrication routes (Naslain, 1992 and 2004); 3) High purity of the matrix deposited by CVI. However, all CVI methods, just like other processing methods, leave a certain amount of void fraction or unfilled porosity in the composite, typically of the order of l-10%. Residual porosity may be open (i.e. accessible from the external surface) or closed, and interconnected or not. Whether and how residual porosity affects the performance of the final product depends on the materials, processing and application.

The use of microwave radiation is a potentially attractive alternative due to its potential for generating a controllable inverse temperature profile during the heating of a ceramic fiber preform (Yin et al., 1997). To this end microwave-heated CVI processes (MWCVI) have been recently developed (Cioni, 2007; Jaglin et al., 2006). Different from conventional heating, this method allows the creation of a temperature gradient from the center of the preform to its periphery (Yin et al., 1997). The surface of the sample can be cooler than the bulk because it releases heat by conduction/convection or radiation to the surrounding atmosphere and to the cavity walls which are much colder because they are built with low dielectric loss materials. Therefore the deposition of the ceramic matrix proceeds from the inside to the outside, avoiding the problems connected with the sealing

of the outer pores of the preform (Jaglin et al., 2006). By means of the MWCVI process high purity and high density SiC matrices can be obtained and preforms of very complex geometry can be successfully infiltrated, at operating temperatures between 900 and 1200°C. Since the pressure required by the process is low (1-100 kPa), the damaging of fibers and their reactions with the matrix are limited. Previous works carried out by Binner et al. (Yin et al., 1997; Timms et al., 2001), based on SiC_f/SiC components (50 mm diameter, 10 mm thick), has shown that by using microwaves to enhance the CVI process, fabrication times can be reduced from hundreds of hours to around 30 hrs.

Together to the advantages, described above, of microwave heating there some technical difficulties associated to the possible insurgence of thermal instabilities (*run-aways*). In fact in multimode applicator, which is more suitable for heating large objects with a complex shape, the intensity of the electromagnetic field varies from point to point due to the formation of stationary waves. This means that a given specimen to be heated received an amount of energy which varies from point to point. This can be the main problem in materials, like ceramics, characterized by low thermal conductivity resulting a non homogeneous distribution of temperature with some points (hot spots) much hotter than surrounding material. Since in many materials dielectric properties increase exponentially with temperature, the hot spots can reach extremely high temperatures even leading to local fusion of the material. These inhomogeneities in local temperature can even give rise to high internal stresses in the material, due to the differential thermal expansion, with formation of cracks and even leading to the fracture of the sample during heating. Therefore, in order to make the most of the microwave heating in this application the prediction of the temperature profile, the electromagnetic field and the prevention of thermal instabilities is of fundamental importance.

Many different numerical schemes have been used to predict the electromagnetic fields in microwave systems. These schemes are based on either the time domain (TD) formulation or the frequency domain (FD) formulation. Numerical techniques to solve Maxwell's equations in the time domain include the transmission-line matrix (TLM) method (Johns and Beurle, 1971), the finite difference time-domain (FDTD) method (Dibben and Metaxas, 1994), the moment method (MOM), line method (MOL), and the finite element time-domain (FETD) method (Yee, 1966). While FDTD has been very widely used in the past, FETD methods have also been developed in recent years (Lee et al., 1997). FETD is an outgrowth of advances in finite-element frequency-domain (FEFD) methods and presents several advantages over FDTD including the use of high-order vector basis functions to achieve high accuracy, unconditional stability to allow the time step to be taken independent of the mesh size, and the use of a single mesh that easily conforms to material interfaces. The use of he Faedo–Galerkin procedure

provides a very natural way for handling field and flux continuity conditions at material interfaces, thus further enhancing modeling accuracy (Lee et al., 1997). Therefore the use of Galerkin formulation offers a unifying approach for the exploitation of a variety of choices of trial functions, some of them more appropriate for specific types of geometries than others. For most materials the dielectric properties widely vary with temperature, so it is very important to predict thermal instabilities (run-away) that may occur during microwave heating. A two-dimensional model has been developed by Midha et al. (Midha and Economou, 1997 and 1998) in order to simulate chemical vapor infiltration of fiber-reinforced composite materials with radio frequency heating. The model equations, including energy transport, multicomponent mass transport, pore structure evolution and the power absorbed by the preform, were solved by a appositely written finite element method to study carbon chemical vapor infiltration in a cylindrical carbon preform.

The objective of this work is the development of an innovative microwave heated chemical vapor infiltration pilot plat in order to produce silicon carbide based ceramic matrix composites. The conventional CVI process was modified and supplemented in order to reduce the CVI process time and to lower the cost of this typically expensive process. In literature a few examples of MWCVI processes are reported but only at laboratory level: an important characteristics of this research is that typical lab-scale technical solutions that are not suitable for industrial production plants, have been carefully avoided in order to easily carry out a scale up of this process. A perspective pilot scale reactor was designed and built, in this work. Two commercial packages were used to predict the temperature profile and the electromagnetic field. A coupled thermal and electromagnetic model was developed, but using commercial software in order to easily apply the model to every type of sample geometry. A specifically developed code was written to couple the thermal and electromagnetic analysis in order to simultaneously estimate the electromagnetic field and the temperature profile inside the reactor with a series of iterative calculation steps.

2. Experimental section

2.1 Experimental apparatus

In order to design and build the new MWCVI system (Fig. 1a and 1b) it was necessary to prepare: a system for generation and transfer of microwave energy to the preform to be heated, a flow system for the reagent and carrier gases in order to bring them in contact with the preform without contamination and in safety conditions, a system for the treatment of exhaust gases, and an advanced electronic apparatus of process control and management.

The Pilot Plant was designed after the thermal and electromagnetic modeling.

a)

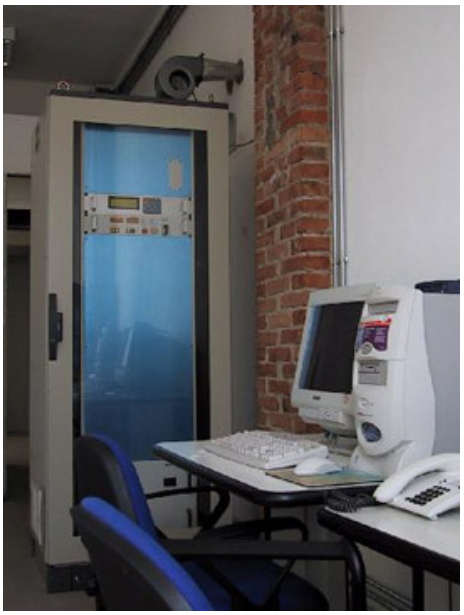

b)

Fig. 1 An image of the MWCVI pilot plant (a) and the control station (b)

2.1.1. The microwave section

The microwave section of the pilot plant consisted of a 6 kW, 2.45 GHz Muegge variable power magnetron connected to the applicator by a rectangular wave guide. A circulator and a dummy water load were used to protect the magnetron from reflected power. A quartz window kept away the inlet from potentially toxic gases into the microwave generation section. A mode stirrer was used to improve the electromagnetic field homogeneity. The tuning of the microwave source with the applicator was carried out by a Muegge autotuner. All the electrical instrumentations close to the reactor (magnetron, autotuner, circulator) were located into a pressurized cabin to avoid potential deflagrations due to casual leakages of explosive gases used in the MWCVI process.

2.1.2. The control system

A computer station enabled the automatic control of the reactor temperature with a feedback loop on the magnetron power generator. The monitoring system allowed also the monitoring of the absorbed and reflected power, the cooling water temperature and the remote activation of the mode stirrer. The control

system automatically disabled microwave generation in case of insufficient or lacking water flow or when the bottom of the applicator-reactor was not fully shut during the experimental trials.

2.1.3. The reactor

The MWCVI reactor (section shown in Fig. 2) was a stainless steel (AISI 304) multi-mode cylindrical applicator, closed at both ends by two flanged disks. The inlet for the premixed reagent gases was located on the lower end. The microwave inlet port was positioned on the upper end. The reactor is provided of a mode stirrer with the function of distribute the electromagnetic field in order to guarantee a homogenous irradiation of the microwaves on the preform. It was necessary to use the most possible irregular shape to limit the possibility of stationary waves and hot spots in the applicator. Then the mode stirrer had manually distorted aluminum wings attached to each branch of the stainless steel cross. It was placed in the space between the closing disc of the inner chamber and the superior extremity of the reactor. Two optical pyrometers were used to control and monitor the temperature of the sample and the insulator. All electrical connections used suitable and deflagrating devices.

2.1.4. The insulator and the preform

The choice of the insulating material used for the inner lining of the reactor was particularly complex. An ideal insulating material needed to both show the characteristics typical of refractory and thermally insulating materials and, at the same time, it had to be transparent to microwaves to avoid thermal losses and even thermal run-away problems. A commercial alumino-silicate fiberboard (Duraboard 1600 from Unifrax, Saronno, I), with dielectric properties similar to mullite, was chosen for the insulation of the reactor.

SiC preforms were obtained using 15-layer Ceramic Grade Nicalon NL 202 (Nippon Carbon Co., LTD. Technical datasheet) woven fabric in the form of bricks of 20x40x80 mm in size. They were located orthogonal to the reactor longitudinal axis, in a refractory inner chamber assembled to create a flow directed through the preform. In the picture (Fig. 2) the arrows show that the reagent gas flow, in principle, can go through the sample thickness and also around the sample. The first layer (layer 1) is the nearest sample surface with respect to the reagent gas flux, the 7^{th} layer (layer 7) is in the center of the composite and the 15^{th} layer (layer 15) is on the upper surface.

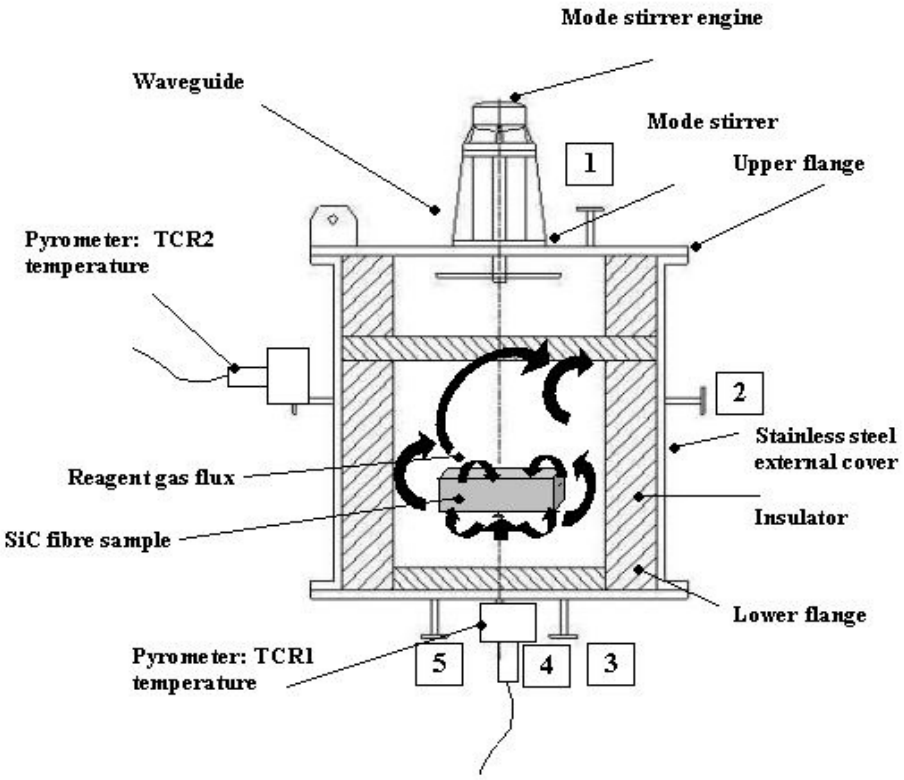

List of metallic gates:

1: Ar flux for the mechanical seal of metallic rotating parts

2: Output of the exhausted gases and reaction products

3-4-5: Input of inert gases (N_2 or Ar) for cleaning

Fig. 2 Section of the MWCVI reactor

2.1.5. Experimental MWCVI trials

Methyltrichlorosilane (MTS, Sigma-Aldrich, 99% of purity)) was used as the precursor material for SiC deposition (Lackey et al., 1998). The MTS gas (boiling point: 66°C) was produced by the vaporization of MTS liquid in a suitable temperature controlled vessel. When heated to around 1000 °C, MTS decomposes into SiC and HCl according to the following reaction:

$$CH_3SiCl_3(g) + H_2(g) \rightarrow SiC(s) + 3HCl(g) + H_2(g)$$

The technical gases used for the MWCVI trials were:

- Argon (Ar): it was used as gas carrier for MTS and H_2 inside the reactor. After the infiltration, it was used in order to eliminate residual H_2 inside the reactor and tubes.
- Nitrogen (N_2): it was used to fluxing the system in the preliminary phase and removing air and moisture
- Hydrogen (H_2): it was necessary in order to prevent the Carbon formation, for thermodynamical reasons (Fischman and Petuskey, 1985).

MTS was carried to the reaction chamber using a mixture composed of 97.2% Ar and 2.8% H_2 as gas carrier, with the gas flow passing through the sample thickness. The configuration chosen for the experiments carried out in this work is the isothermal and isobaric chemical vapor infiltration. Respect to the literature (Yin et al., 1997; Timms et al., 2001; Jaglin et al., 2006) the MWCVI pilot plant developed in this work presents the important characteristic of carefully avoiding typical lab-scale technical solutions, like the use of large components in quartz or other materials that are not suitable for industrial production plants, in order to easily carry out a scale up of this process.

The MTS concentration could be controlled by the gas flow rate within the range 10-20 mol/hr, maintaining the MTS liquid at range of temperature between 30°C and 40°C. The molar H_2/MTS ratio was chosen between 500-1000. The total pressure of the reaction chamber was adjusted to 1.01 bar and the products of the reaction were removed with a scrubber system consisting of an aqueous solution of sodium hydroxide (Carlo Erba reagents, 97% of purity) with a concentration of 15 g/l. The standard MWCVI process conditions applied during the experimental trial are summarized in Table 1.

The residual gas (including H_2 and Ar and MTS unreacted decomposition products) are vented into a fume head. At the end of infiltration, the MTS-H_2 stream and microwave power were shut off and argon was allowed to flow through the reaction vessel for a minimum of 2 hr until the sample had cooled down to room temperature and the toxic by-products were completely removed and neutralized.

Table 1 Standard MWCVI Process Conditions

Preform control temperature (°C)	1000-1050
Total Pressure (bar)	1.01
MTS reservoir temperature (°C)	30-40
Hydrogen gas flow rate (mol/hr)	180
Argon gas flow rate (mol/hr)	6250
MTS fraction at inlet (voll. %)	0.15-0.30
Molar H_2/MTS ratio	500-1000

A schematic diagram of the MWCVI system used to infiltrate the silicon carbide fiber preforms is reported in Fig. 3.

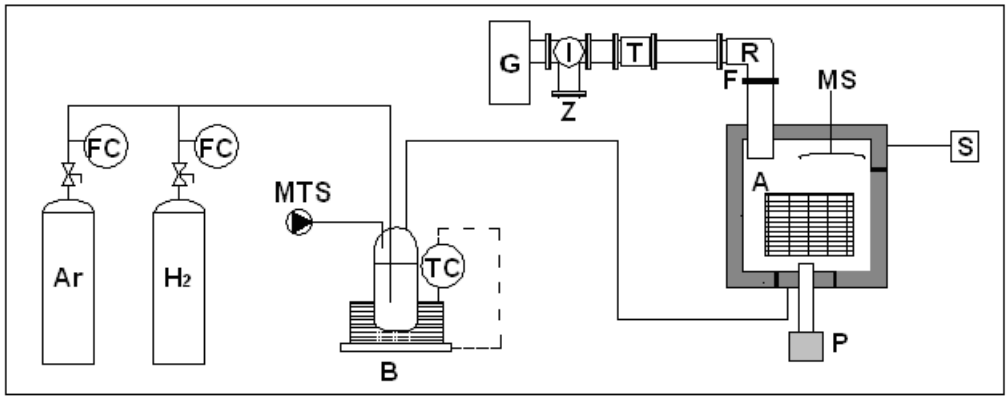

Fig. 3 Scheme of the MWCVI reactor (G: generator 2.45 GHz, 6 kW; I: three port circulator; Z: water cooled dummy load; T: auto tuner; R: connected transition; F: quartz window; A: applicator; MS: mode stirrer; P: pyrometer; S: scrubber system; B: bubbler; FC: feed controller; TC: temperature controller)

2.2 Measurements of the reflection coefficient

The reflection coefficient S was measured by means of a Rohde&Schwarz ZVRE Network Analyzer in the 40MHz÷1GHz range and compared with values obtained by the electromagnetic model.

The wave components required to the definition of *S* are shown in Fig. 4. The wave components from the gate *n* at the inlet and outlet, respectively a_n and b_n, are defined in Equation (1), where n=1, 2:

$$a_n = \frac{V_n^+}{\sqrt{Z_0}} \qquad b_n = \frac{V_n^-}{\sqrt{Z_0}} \tag{1}$$

Where V_n^+ and V_n^- are voltages measured respectively at the inlet and at the outlet of the gate *n*. The other parameters are defined as following:

$$S_{11} = \frac{b_1}{a_1} \qquad S_{12} = \frac{b_1}{a_2} \qquad S_{21} = \frac{b_2}{a_1} \qquad S_{22} = \frac{b_2}{a_2} \tag{2}$$

The ratio b_1/a_1 is known as reflection coefficient, while b_2/a_1 is known as transmission coefficient because it relates the wave ingoing into the gate with the one outgoing the system.

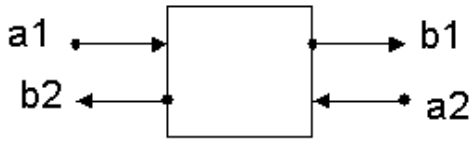

Fig. 4 Parameters for the determination of the reflection coefficient S

3. Modeling

The analysis of the microwave electromagnetic field was carried out using a commercial 3D full-wave FETD software, Ansoft HFSS, version 8.0.25 (Ansoft, 2001). The Abaqus 5.8 F.E.M. package (Abaqus, 1998) was used to perform the thermal modeling. Both software packages were run using a AMD Athlon MP2000+ workstation operating at 1.667 GHz. The resolution of the EM problem with Ansoft HFSS does not account for thermal gradients in the material, so the temperature dependence of the dielectric parameters cannot normally be taken into consideration. This inconvenience has been circumvented by dividing the insulating material and the SiC preform into a series of finite elements each of which of a different set of dielectric constants.

A specifically developed Fortran code was written to evaluate, from the temperature profile computed from Abaqus, the mean temperature of each finite element, used by Ansoft HFSS, and the corresponding real and imaginary part of the dielectric constant. In this way a sort of "dielectric constant profile" was obtained using $\varepsilon'(T)$ and $\varepsilon''(T)$ experimental data for mullite and SiC obtained from the literature (Goodson, 1997). Once the electric field, E, was calculated from Ansoft HFSS for each finite element, another specifically developed Fortran code was used to compute the dielectric heat generation ($\dot{q}_d$) inside every element from the Equation (3):

$$\dot{q}_d = 2\pi f \varepsilon_0 \varepsilon''(T) \left|E\right|^2 \tag{3}$$

where f is the frequency and ε_0 is the permittivity *in vacuo*.

The total heat ($\dot{q}_{tot}$) was given by the sum of the dielectric heat generation and the irradiation heat ($\dot{q}_i$) in Equation (4):

$$\dot{q}_i = C\left[\left(\theta_A - \theta^Z\right)^4 - \left(\theta_B - \theta^Z\right)^4\right] \tag{4}$$

where:

$$C = \frac{F\sigma}{\frac{1}{\varepsilon_A} + \frac{1}{\varepsilon_B} - 1}$$

$\dot{q}_i$ is the irradiation heating flux per surface unit

ϑ_A, ϑ_B and ϑ^Z are respectively the temperature of surface A, surface B and the absolute temperature

σ is the Stefan-Boltzman constant

ε_A and ε_B are respectively the emissivity of surface A and surface B

F is the effective factor of view.

The procedure was iteratively repeated until a constant temperature was obtained for each element. The sample, the reactor, the wave guide, the mode stirrer and the insulator were modeled by meshing the structure, as shown in Fig. 5a). In Fig. 5b) a scheme of the iterative modeling procedure is reported. The start point was a preliminary thermal analysis by means of Abaqus. At first a temperature profile was obtained, by fixing the initial and boundary conditions. The boundary conditions were 20°C for the atmosphere surrounding the sample, while the initial conditions for the SiC preform were 1200°C (maximum value of the temperature reachable by the sample).

Consequently the nodal temperatures were acquired, and it was necessary to calculate the mean temperatures and hence the resulting dielectric properties of the elements in which the insulator was divided for the EM analysis. Then the magnetic field inside the reactor and the value of the electric field were outlined in each node by Ansoft HFSS. Finally the heating flux due to the electric field associated to each node was calculated and it was used as input for the Abaqus program and a iterative procedure was started. The condition of constant temperature was taken as satisfied when the difference of mean temperature for each element obtained from two different iterations was less then 2°C.

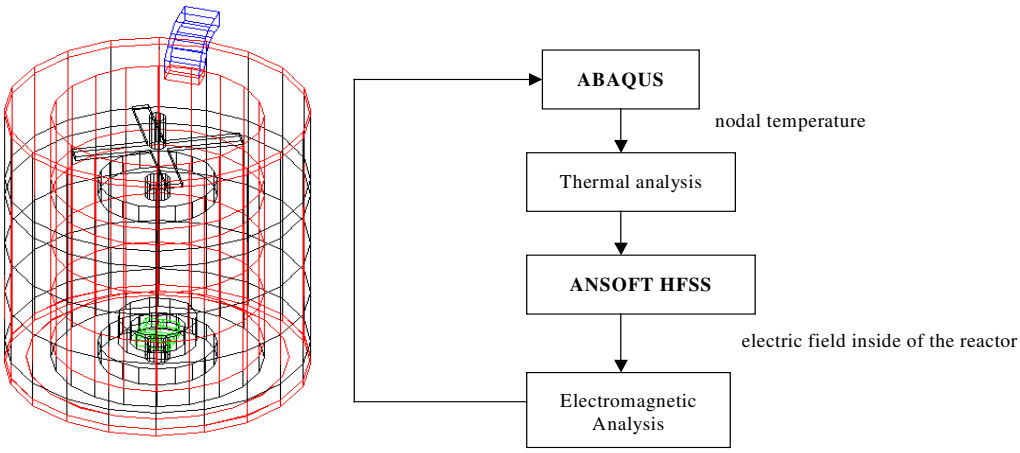

Fig. 5 Modeling of the MWCVI reactor (a) and scheme of the iterative modeling procedure (b)

Regarding to the modeling of the mode stirrer, it is necessary to point the attention on some important elements. Although mode stirring has been used for many years, very little research has been carried out into modeling or optimizing the design of the mode stirrer. Recently the use of genetic algorithms has been examined to enhance stirrer design (Clegg et al., 2005). However the modeling of a stirrer inside a chamber is very time consuming as each stirrer position requires a separate run of the model. So, in this case the mode stirrer was designed by 'rule of thumb'. In this work, the mode stirrer was manually distorted aluminum wings attached to each branch of the stainless steel cross. The simulation and the measurements were carried out for different angles with respect to the microwave inlet port, 0°, 30° and 60° in order to reproduce the effects of the rotation of the mode stirrer.

4. Results and discussion

4.1 Modeling

4.1.1. Thermal modeling

Thermal modeling enabled the evaluation of the average temperature inside different zones of the MWCVI reactor. The electromagnetic field did not significantly alter the temperature profile, so the high temperatures reached in some nodes of the insulator could be attributed to the irradiated heat from the preform. The highest temperatures were reached in a zone under the preform and in the area above to the preform itself (Fig. 6). The temperature profile of the insulator resulted quite uniform and with acceptable values.

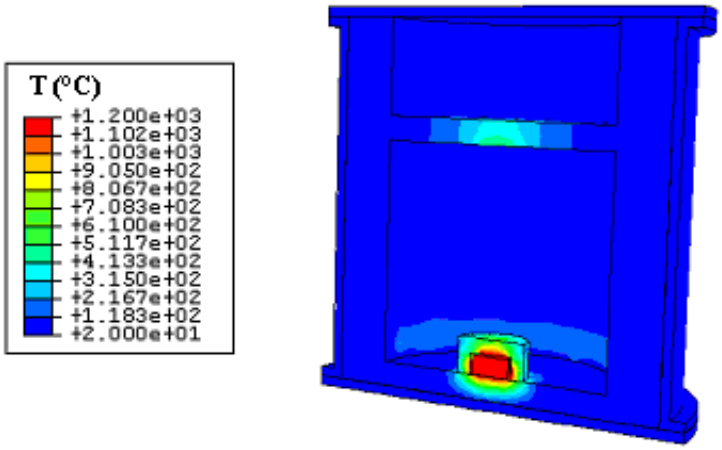

Fig. 6 Modeling results after the thermal analysis

4.1.2. Electromagnetic modeling

The aim of electromagnetic modeling was to evaluate the electromagnetic field inside the reactor and to verify its homogeneity in the insulator and in the preform, because a uniform electromagnetic field involved a homogeneous distribution of temperature and therefore a uniform MTS deposition. Then the electric field was determined in the preform and in the insulator. Ansoft HFFS gave the electric fields values in the nodes for different angles of mode stirrer, enabling the calculation of the mean value of the field in each element. In Fig. 7 the results from the electromagnetic modeling are reported, respectively for 0° (a), 30° (b) and 60° (c) of the angle of rotation of the mode stirrer. Values of electric field belonging to the same plane are quite comparable meaning that the electromagnetic field, even if it continuously changed during the rotation of mode stirrer, showed only small fluctuations around the average value.

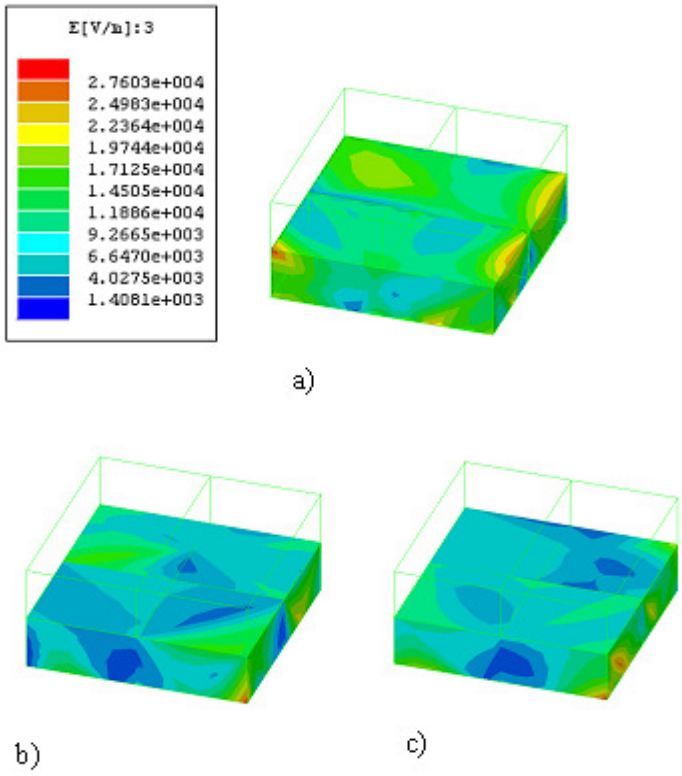

Fig. 7 Results of modeling for electromagnetic field in the preform for 0°(a), 30° (b) and 60° (c) of mode stirrer

The different values of electric field assumed in several planes, may be due to the planarity of modeled mode stirrer that is not capable to fluster the electric field along Z axis and this could be solved by using the real mode stirrer. The electromagnetic field was rendered more homogeneous by employing the mode stirrer, in fact without it the field could assume dissimilar values with a sinusoidal mode, with the undesired consequence of a non uniform deposition of MTS during infiltration phase.

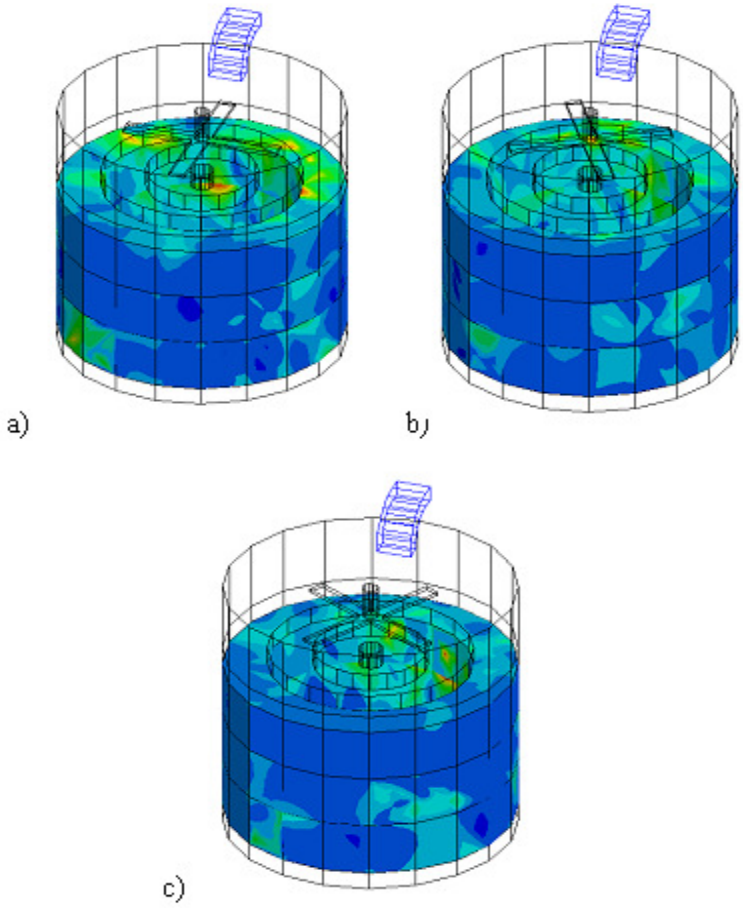

Fig. 8 Results of modeling for the electromagnetic field inside the insulator for 0°(a), 30° (b) and 60° (c) of mode stirrer

Fig. 8 shows that the mean value of the electromagnetic field in the insulator is lower or comparable with the related values calculated in SiC preform, except in some planes, in which values are higher. The planes nearest to the inlet of microwaves presented the highest values of electromagnetic field. That is probably due to the mode stirrer that was not able to disperse the electromagnetic

waves along the reactor axis, with the consequent accumulation of waves on the plane surfaces. Then the insulator could warm up, but slightly, because the heating of some points where the electric field was increased was well compensated by the big volume of the insulator.

4.2 Experimental results

4.2.1. Reflection coefficient measurements

In Fig. 9 S_{11} parameter is reported as function of frequency in the range of 2.44-2.46 GHz. The shape used for the mode stirrer (m.s.) effectively used in our MWCVI trials was too complex to be modeled with a fine element code like Ansoft HFSS. In fact it is necessary to use the most irregular shape possible to limit the possibility of stationary waves and hot spots in the applicator. Therefore, to the purpose of model validation, it was decided to compare the experimental S_{11} data obtained with a m.s. with a simplified shape (in the form of a simple cross in stainless steel) with the values calculated by Ansoft HFSS. Moreover the experimental data for the simplified m.s. were also compared with that obtained in the case of the real mode stirrer. In order to reproduce the effects of the rotation of the mode stirrer, both the simulation and the measurements were performed for three different angles, with respect to the microwave inlet port, 0° (Fig. 9a), 30° (Fig. 9b) and 60° (Fig. 9c). This choose was made firstly because the stirrer was symmetric and secondly because the rotation speed of the mode stirrer (about 50 rpm) was significantly lower than the frequency of the electromagnetic field (2.45 GHz).

The differences observed between the curves could be attributed to the fact that the material data used for modeling were quite different from that used in the real reactor and there could be imperfections that consequently increased or decreased the microwave absorption. Moreover the model did not consider the presence of nozzles. Taking into account these consideration, the agreement between the computed and measured S_{11} data for the simplified m.s. is quite satisfactory, thus validating the model. Data obtained from network analyzer showed lower values of S_{11} in case of the real mode stirrer that confirmed the need of a mode stirrer with a very complex shape in order to minimize the reflected power and then produce a more homogeneous electromagnetic field.

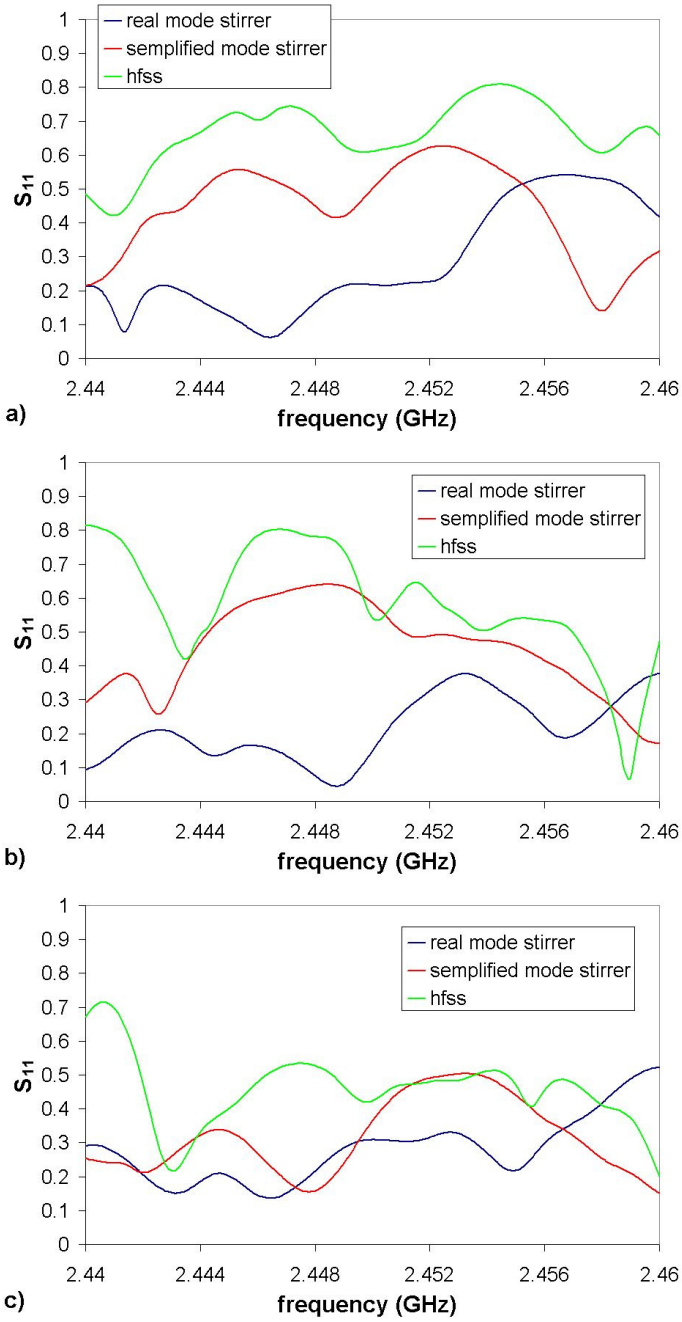

Fig. 9 S_{11} parameter as function of frequency in the range of 2.44-2.46 GHz [hfss: modeling data for simplified m.s.: experimental data for simplified m. s., experimental data for real m.s.: real mode stirrer oriented with angles of 0° (a), 30° (b) and 60° (c)]

4.2.2. MWCVI trials

In Fig. 10 is reported a typical temperature profile recorded during an experimental infiltration trial. The Nicalon fibrous preform was infiltrated for about 18 hours subdivided in four consecutive trials each with duration of 4.5 hr. Temperature is measured by an optical pyrometer placed under the Nicalon preform. About 3.5 kW of microwave power was required to heat the sample until the temperature of 1000°C in only 30 minutes, because of the high dielectric constant of silicon carbide. At this point MTS was allowed into the chamber to start the infiltration. The sample temperature was maintained constant (temperature of reaction) by the action of a PID controller that adjusted the power in order to keep the temperature constant.

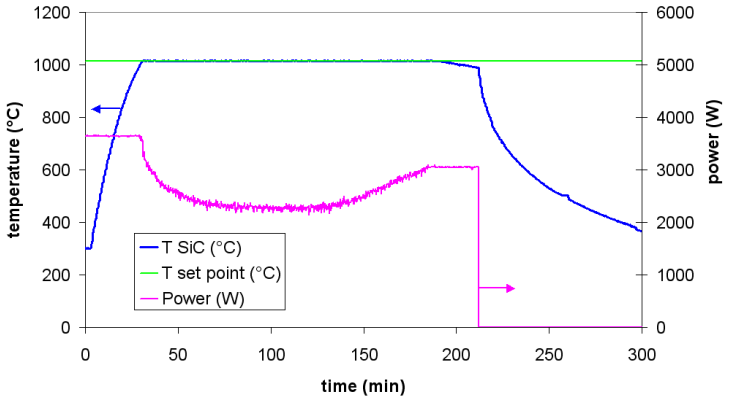

Fig. 10 Temperature profile for microwave chemical vapor infiltration of SiC$_f$/SiC sample.

The densification rate of 15-layer fiber preform is shown in Fig. 11a) as a function of the MTS molar flow rate. It is clear that the densification rate enhanced with the increase of the reagent molar flux. In Fig. 11b) the weight increase vs. time is reported, showing that about 18 hr are needed to reach the 70% of weight increase, with an average MTS molar flux of 15 mol/hr. Therefore the overall deposition of silicon carbide from the MWCVI process was resulted a linear function of the time.

The layer 1 (Fig. 12a)), directly in contact with the reagent gas flux, resulted almost completely infiltrated with no visible porosity observed at SEM. This lower surface appeared more dense and compact. This type of deposition is not desirable since it can make the proceeding of the infiltration difficult if not impossible, due to the sealing of the outer pores of the preform.

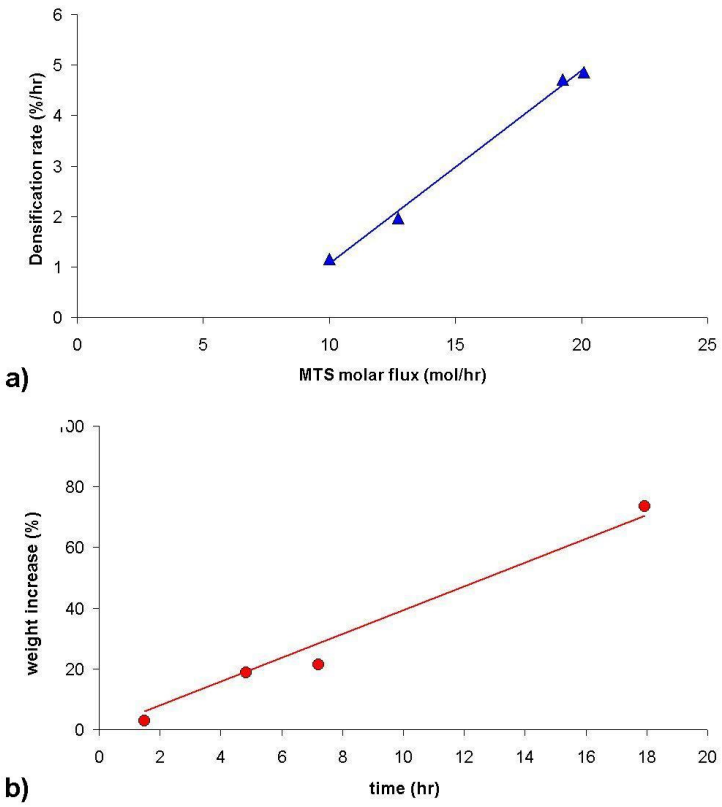

Fig. 11 Densification rate of 15-layer fiber preforms as a function of the MTS molar flux, during a multi-cycles process of 18 hr (a) - Weight increase (%) vs. time during a multi-cycles process of MWCVI, with an average MTS molar flux of 15 mol/hr (b).

Fig. 12b) presents a SEM micrograph at 1500 x magnification of the section of the layer 4 of the SiC_f/SiC composite surface after the microwave assisted infiltration. Although a certain increase in the diameter of the fibers were occurred, the composite contained an evident inter-tow porosity. Then the upper surface resulted more infiltrated than the inner layers. This effect is probably due to the fact that a portion of the gaseous reactive mixture bypassed the sample, flowing around it, filling up the chamber and infiltrating the sample from the opposite side respect to the inlet flux. In other terms, the mechanism of deposition in the outer layers was mostly due to convective mass transfer while in the inner layers only diffusion can take place during the infiltration. Comparing the surface layer with the more inner layer it is evident that, for the upper surface, the process was comparatively slower, resulting in a higher degree of porosity. Nevertheless the deposition resulted quite uniform with a large number of spherical micro

crystals on the fiber surface as showing in Fig. 13a) in comparing with the untreated Nicalon fibers (Fig. 13b).

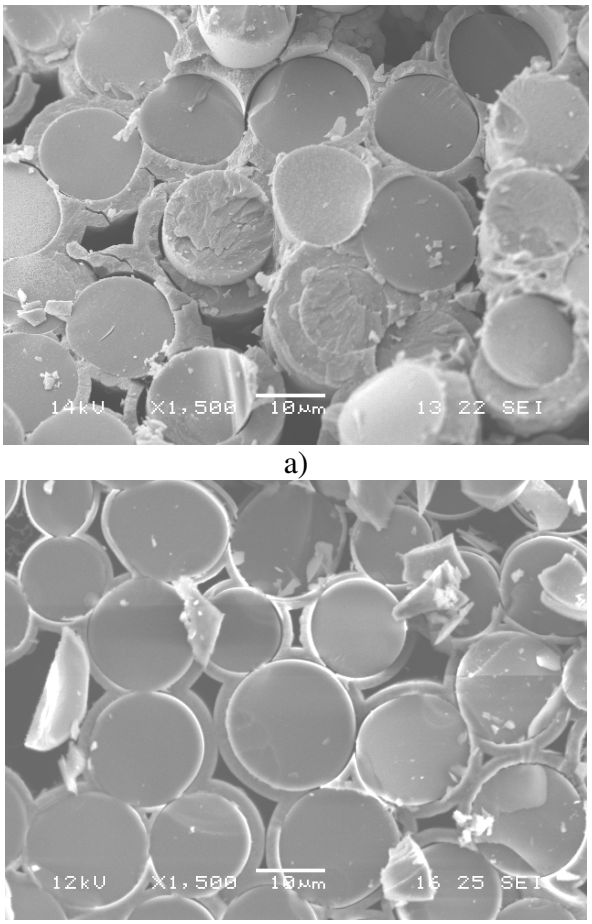

a)

b)

Fig. 12 SEM image showing sections of the SiC_f/SiC sample under 1500 x magnification in the layer 1 (a) and layer 4 (b).

These experimental evidences were apparently in disagreement with the results obtained by Jaglin (D. Jaglin, 2002) where a preferential densification of the SiC_f/SiC composites occurred from the inside out. In that case the inverse temperature profiles that could be produced via microwave heating was fully exploited. However, in this work the experimental apparatus used did not allow for temperature measurements inside the sample, but only in its surface. This means that the only indication that an inverse temperature profile had been attained, during the microwave heating, would have been the observation of a larger degree of SiC deposition on the fibers located in the bulk of the sample.

This occurrence was not appreciated, but this does not rule out the possibility that an inverse temperature profile had really been attained. We believe that the reason why we observed a larger deposition on the outer surface nearer to the gas inlet is that the gas reagent flux was probably not well optimized. In fact MTS went straight against the lower surface of the composite and there it decomposed mainly by filling the more external pores present on the first layers. The gas mixture progressively decrease its content in reactive component (MTS) and also reaches the upper surface with a reduced mass flow rate. This can explain the reduced deposition observed for the outer layer. In general it is evident that, for the outer and the inner layers, the most of the inter- and intra-tow porosities were not fully infiltrated and sealed. However this fact is known also for composites produced with standard CVI, which generally contain macroscopic inter-fiber bundle pores which hamper several important properties related with composite rigidity and transport properties.

Further MWCVI cycles will be needed in order to completely densify the preform, but, in order to further reduce the processing time, a future development of this research may be the combination of MWCVI with polymer impregnation and pyrolysis (PIP) (Nannetti et al., 2002; Donato et al., 1998) process for the preparation of SiC_f/SiC composites. The PIP process could be only a possible pre-treatment of the fibers in order to densify the preforms and finally CVI could be used to obtain a final SiC coating on the preforms densified. In this way it will be possible to considerably reduce the time to infiltrate the macro-pores that exist between the fiber tows. These can be hundreds of micrometers wide and consequently infiltrate much more slowly than the micropores that exist between the fibers within the tows.

Fig. 14 shows the XRD patterns of composites SiC_f/SiC after a MWCVI treatment with duration of 18 hr, respectively for the outer layer (Fig. 14a) and the inner layer (Fig. 14b). The SiC_f/SiC composites resulted evidently crystalline and composed of a single β-phase. The absence of a large peak centered at about 22° in all XRD patterns of MWCVI produced composites suggested the lack of amorphous SiO_2 (Kholmanov et al., 2002). Therefore the oxygen content in the MWCVI treated sample was considerably decreased respect the untreated fibers. This means that the plant was well-sealed and suitable in order to carried out operations in absence of moisture and air, which maybe responsible of silica and formation of compounds of silicon carbide affected by oxygen impurities. The sensible decrease of oxygen content in the obtained composite can be considered an important result because the high temperature mechanical properties of SiC_f/SiC composites get considerably worse when oxygen is present in the material.

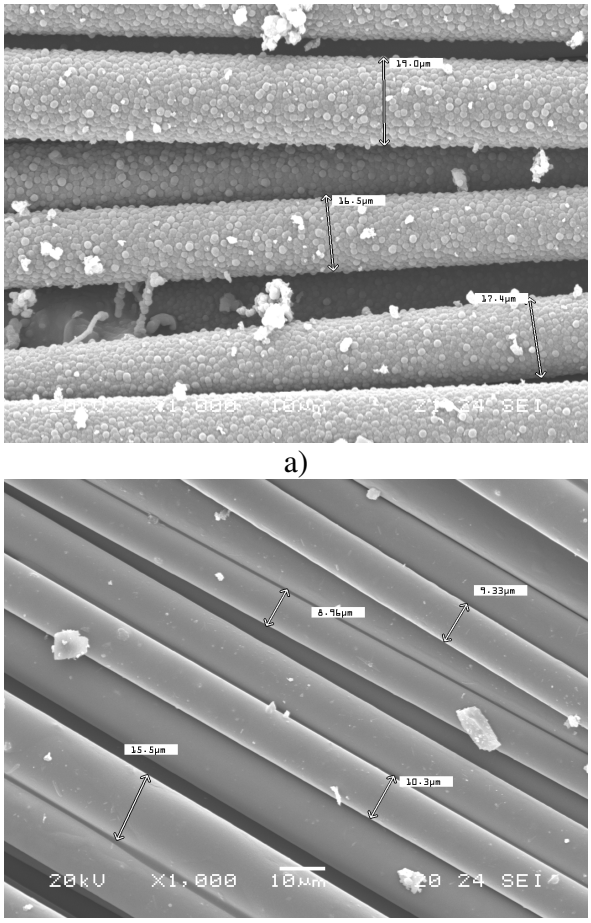

Fig. 13 SEM image at 1000 x magnification showing the silicon carbide deposits produced via MWCVI of the same fibers (a) and the untreated Nicalon fibers (b)

The crystalline phases were identified on the basis of XRD patterns of α-silicon carbide and β-silicon carbide reported in literature (Zhu et al., 1998; Tanaka et al., 2001) and they were evidenced in the same way either on the surface of the SiC_f/SiC composite (layer 1) either in the inner part of the sample (layer 4). The synthesis of β-SiC powders requires the use of temperatures lower than 1700°C because the β polytype (face-centered cubic crystal structure) is metastable, and it tends to transform to α polytypes (hexagonal or rhombohedral) at higher temperatures (Xu et al., 2001). Instead beta modification (β-SiC), with a face-centered cubic crystal structure, is formed at temperatures of below 2000 °C and it is reasonable that it can be found in composites produced in these work, where the maximum temperature measured was 1050°C. There was no evidence of alpha silicon carbide (α-SiC, with the typical hexagonal crystal structure)

because it is known that it is formed at temperatures greater than 2000 °C (Ortiz et al., 2001).

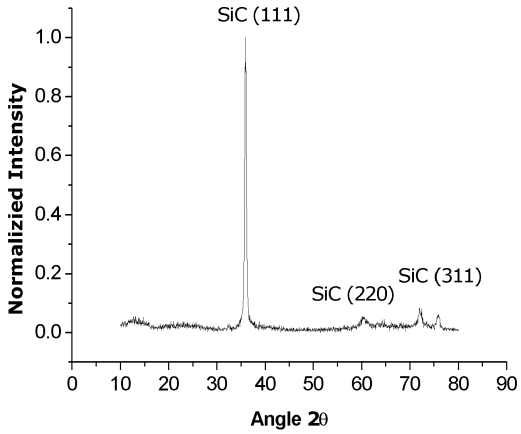

a)

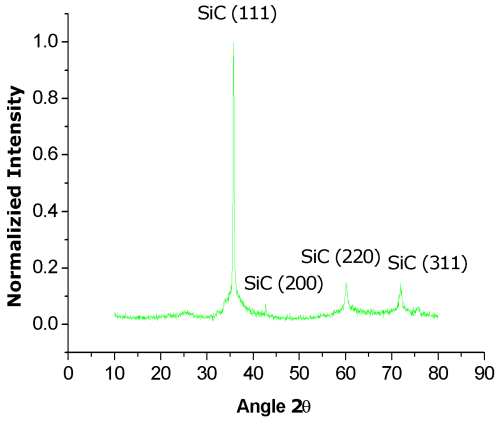

b)

Fig. 14 XRD pattern of layer 1 (a) and layer 4 (b) of MWCVI treated SiC sample

5. Conclusions

Results obtained from the coupled thermal and electromagnetic model developed in this work showed a relatively constant electric field inside the sample, and a rather uniform heating. The simulation results showed a negligible heating inside the chosen insulator. The temperature and electric field were reasonably constant in the sample, allowing a uniform heating when, in order to improve the process efficiency, a mode stirrer is used to achieve a better distribution of microwave power. An uniform deposition of MTS on silicon carbide fibers predicted by this

result was confirmed by the experimental evidences. In fact an average weight increase of about 70% respect to the initial sample was achieved in 18 hr of microwave treatment. The silicon carbide deposition inside the sample was sufficiently homogeneous and compact, with an evident inter-tow porosity was still present. The densification of the SiC_f/SiC composites results deeper from the lower to the upper surface, because the gas reagent flux was not yet well optimized. However the results obtained during these MWCVI trials suggest that the optimal heating, the deposition patterns predicted for microwave heating and the reduced infiltration times are successfully achievable. Therefore this work can be considered a first pioneering step towards the development of an innovative MWCVI pilot plant.

Notation

$\dot{q}$	dielectric heat generation flux
a	wave components from the gate n at the inlet
b	wave components from the gate n at the outlet
E	Electrical field
f	frequency
S	reflection coefficient
T	Temperature
V-	voltages measured at the outlet of the gate n
V+	voltages measured at the inlet of the gate n

Greek Letters

ε	permittivity

Subscripts

0	vacuum
i	irradiation
d	dielectric
n	Gate

References

Abaqus Version 5.8 “Theory manual”, (1998), Hibbitt, Karlsson & Sorensen, Inc. Pawtucket, RI.

Anastas, P.T., Warner J.C., (1998), “Green chemistry theory and practice”, Oxford University Press, New York.

Ansoft HFSS Version 8.0 Manual, "Getting started: an eigenmode problem, Ansoft corporation", (2001), Pittsburgh, PA.

Besmann, T.M., Mclaughlin, J.C., Lin H.T., "Fabrication of ceramic composites - forced CVI", J. Nucl. Mater., (1995), Vol. 219, 31-35.

Chawla, K.K., "Ceramic matrix Composites", (1993), Chapman & Hall.

Cioni, B., "Application of microwave energy in innovative chemical engineering and materials science processes", (2007), PhD thesis, Pisa, Italy.

Clegg, J., Marvin, A.C., Dawson, J.F., Porter, S.J., "Optimization of stirrer designs in a reverberation chamber", IEEE Transactions on Electromagnetic Compatibility, (2005), Vol. 47, N° 4, 824-832.

Dibben, D.C., Metaxas, A.C., "Finite element time domain analysis of multimode applicators using edge elements", J. Microwave Power E.E., (1994), Vol. 29, No. 4, 242-251.

Donato, A., Nannetti, C.A., Ortona, A., Borsella, E., Botti, S., Casadio, S., D'Alessandro, G., Licciulli, A.A., Martelli, S., Masci, A., "Process for producing ceramic matrix composites by liquid infiltration", (1998), US Patent 5853653.

Fischman, G.S., Petuskey, W.T., "Thermodynamic analysis and kinetic implications of chemical vapor deposition of SiC from SiC-C-Cl-H gas systems", J. Am. Ceram. Soc., (1985), Vol. 68, No. 4, 185-190.

Goodson, C.C., "Simulation of microwave heating of mullite rods", (1997), PhD thesis, Virginia Tech.

Gulden, T.D., Kaae, J.L., Norton, K.P., Thompson, L.D., Spear, K.E., Cullen, G.W., "Forced-flow thermal-gradient chemical vapor infiltration (CVI) of ceramic matrix composites", Proceedings of Eleventh International Conference on Chemical Vapor Deposition, CVD-XI, Seattle, Washington, (1990), Vol. 90, No, 12, 546-552.

Jaglin, D., "Densification of SiC_f/SiC composites via microwave enhanced chemical vapor infiltration", (2002), PhD thesis, Nottingham, United Kingdom.

Jaglin, D., Binner, J.G.P., Vaidhyanathan, B., Calvin, P., Prentice, C., Shatwell, B., Grant, D., "Microwave heated chemical vapor infiltration: densification mechanism of SiC_f/SiC composites", J. Am. Ceram. Soc., (2006), Vol. 89, No. 9, 2710-2717.

Johns, P.B., Beurle, R.L., "Numerical solution of two-dimensional scattering problems using a transmission line matrix", Proc. Inst. Electr. Eng., (1971), Vol. 118, No. 9, 1203-1208.

Katoh, Y., Dong, S.M., Kohyama, A., "Thermo-mechanical properties and microstructure of silicon carbide composites fabricated by nano-infiltrated transient eutectoid process", Fusion Eng. Des., (2002), Voll. 61-62, 723-731.

Katoh, Y., Kohyama, A., Nozawa, T., Sato, M., "SiC/SiC composites through transient eutectic-phase route for fusion applications", J. Nucl. Mater., (2004), Voll. 329-333, No. 1, 587-591.

Kholmanov, N., Kharlamov, A., Barborini, E., Lenardi, C., Li Bassi, A., Bottani, C.E., Ducati, C., Maffi, S., Kirillova, N.V, Milani, P., "A simple method for the synthesis of silicon carbide nanorods", J. Nanoscience and Nanotechnology, (2002), Vol. 2, 453-456.

Lackey, W.J., Vaidyaraman, S., Beckloff, B.N., Moss T.S., Lewis, J.S., "Mass transfer and kinetics of the chemical vapor deposition of SiC onto fibers", J. Mater. Res., (1998), Vol. 13, No. 8, 2251-2261.

Lee, J.F., Lee, R., Cangellaris, A., "Time-domain finite-element methods", IEEE Trans. Antennas Propagat., (1997), Vol. 45, No. 3, 430-442.

Lovell, D.R., "Carbon and high performance fibers" Directory, (1991), 5th edn., Chapman and Hall, London.

Midha, V., Economou, D.J., "A two-dimensional model of chemical vapor infiltration with radio frequency heating", Journal of The Electrochemical Society, (1997), Vol. 144, No. 11, 4062-4071.

Midha, V., Economou, D.J., "A two-dimensional model of chemical vapor infiltration with radio-frequency heating - II. Strategies to achieve complete densification", J. Electrochem. Soc., (1998), Vol. 145, No. 10, 3569-3580.

Nannetti, C.A., Riccardi, B., Ortona, A., La Barbera, A., Scafè, E., Vekinis, G. J., "Development of 2D and 3D Hi-Nicalon fibers/SiC matrix composites manufactured by a combined CVI-PIP route", J. Nucl. Mater., (2002), Vol. 307-311, No. 2, 1196-1199.

Naslain, R., "CVI-composites ", in "Ceramic matrix composites", R. Warren, Ed., Blackie, Glasgow, (1992), Vol. 8, 199-244.

Naslain, R., "Design, preparation and properties of non-oxide CMCs for application in engines and nuclear reactors: an overview", Comp. Sci. Technol., (2004), Vol. 64, No. 2, 155-170.

Ortiz, A.L., Sànchez-Bajo, F., Cumbrera, F.L., Guiberteau, F., "X-ray powder diffraction analysis of a silicon carbide-based ceramic", Mater. Lett., (2001), Vol. 49, No. 2, 137–145.

Sheppard, L.M., "Manufacturing ceramics with microwaves? The potential for economical production", Am. Ceram. Soc. Bull., (1988), Vol. 67, No. 10, 1656-1661.

Tanaka, S., Sugimoto, S., Li, J.F., Watanabe, R., Esashi, M., "Silicon carbide micro-reaction-sintering using micromachined silicon molds", J. Microelectromech. Syst., (2001), Vol. 10, No. 1, 55-61.

Timms, L.A., Westby, W., Prentice, C., Jaglin, D., Shatwell, R.A., Binner, J.G.P., "Reducing chemical vapor infiltration time for ceramic matrix composites", Journal of Microscopy, (2001), Vol. 201, No. 2, 316-323.

Xu, H., T. Bhatia, S. A. Deshpande, N. P. Padture, A. L. Ortiz, F. L. Cumbrera, "Microstructural evolution in liquid-phase-sintered SiC: I, effect of starting SiC powder", J. Am. Ceram. Soc., (2001), Vol. 84, No. 7, 1578-1584.

Yee, K.S., "Numerical solution of initial boundary value problem involving Maxwell's equations in isotropic media", IEEE Trans. Antennas Propag., (1966), Vol. 14, N° 3, 302-307.

Yin, Y., J.G.P. Binner, T.E. Cross, "Microwave assisted chemical vapor infiltration for ceramic matrix composites", Ceram. Trans., (1997), Vol. 80, 349-356.

Zhu, Y.Q., Sekine, T., Kobayashi, T., Takazawa, E., "Shock-induced phase transitions among SiC polytypes", J. Mater. Sci., (1998), Vol. 33, No. 24, 5883-5890.